Available online at www.sciencedirect.com

ScienceDirect

Mendeleev Commun., 2018, **28**, 66–69

Mendeleev Communications

Self-organization and properties of dispersed systems based on dilute aqueous solutions of (*S*)- and (*R*)-lysine

Irina S. Ryzhkina,*[a] Svetlana Yu. Sergeeva,[a] Yuliya V. Kiseleva,[a] Alina P. Timosheva,[a] Olga A. Salakhutdinova,[a] Maxim D. Shevelev[a,b] and Alexander I. Konovalov[a]

[a] *A. E. Arbuzov Institute of Organic and Physical Chemistry, Kazan Scientific Center, Russian Academy of Sciences, 420088 Kazan, Russian Federation. Fax: +7 843 273 1872; e-mail: ryzhkina@iopc.ru*

[b] *Institute of Chemistry, Kazan Federal University, 420008 Kazan, Russian Federation*

DOI: 10.1016/j.mencom.2018.01.022

In a concentration range of 1.0–1.0 × 10^{-17} mol dm^{-3}, aqueous systems based on (*S*)- and (*R*)-lysine vary in the ability to form a dispersed phase (domains and nanoassociates) hundreds nanometers in size with different UV absorption spectra of these systems.

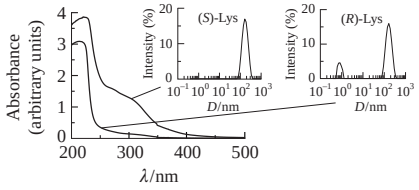

The nonmonotonic concentration dependence of the effects of highly diluted aqueous solutions (1.0 × 10^{-20}–1.0 × 10^{-6} mol dm^{-3}) of biologically active compounds (BACs) attracts considerable attention. However, the application of this phenomenon in pharmacology and medicine is limited by the lack of an explanation of its physicochemical nature.[1]

Recently, based on experimental data,[2,3] it was hypothesized that the nonmonotonic response of biosystems to the effect of highly diluted BAC solutions, the effect of silent zones and the bioeffect sign reversal (hormesis) can be explained by the fact that so-called highly diluted solutions are nanoheterogeneous dispersed systems that undergo a supramolecular domain[4,5]–nanoassociate[2,3] rearrangement in the disperse phase on dilution, which is accompanied by changes in the physicochemical and biological properties of the system.

The nanoassociates[2,3,6,7] are fractal objects hundreds of nanometers in dimension that are formed in dilute aqueous and aqueous-organic systems and involve solute and solvent molecules. They have an electrically charged interface and enhanced viscosity in comparison with the dispersing medium. Domains are generally formed at calculated concentrations of 1–10^{-5} mol dm^{-3}, while nanoassociates are formed at much lower concentrations of 10^{-6}–10^{-20} mol dm^{-3}.

One of the main differences between domains and nanoassociates is that domains are formed both in the presence and in the absence of low-frequency background electromagnetic fields (hypoelectromagnetic conditions).[2,3] Water and aqueous solutions are very sensitive to the impact of weak physical and chemical factors.[8,9] Most likely, it is owing to the fundamental phenomenon that nanoassociates have the unique capability to be formed in the presence of low-frequency electromagnetic fields even at ultra-low BAC concentrations.

Currently, experimental[4,10] and theoretical[8,11] studies of the domains and nanoassociates and their role in the operation of complex biological systems are in progress. The effect of the chemical and spatial BAC structure on the self-organization of aqueous systems is of importance. Therefore, we studied the self-organization and properties of aqueous systems based on α-amino acids[12] and structures containing their fragments.[13] All α-amino acids found in living organisms, except for glycine, are optically active and have enantiomeric L- and D-forms or, in terms of absolute configuration, (*S*)- and (*R*)-forms.[14] The enantiomers not only have different spatial structures of molecules but also show pronounced distinctions in their biological properties due to differences in permeation through biomembranes, in reactions with enzymes, *etc.*[14,15]

In this work, we used dilute (1.0–1.0 × 10^{-18} mol dm^{-3}) aqueous solutions of (*S*)- and (*R*)-lysine (Lys) (**1** and **2**), an essential proteogenic amino acid with a side chain protonated in a neutral pH range,[14] as test materials. (*S*)-Lys has a broad spectrum of biological activity (including the synthesis of antibodies, hormones and enzymes, collagen formation and restoration of tissues) and affects the nervous and immune regulatory systems. The low-concentration solutions of (*S*)-Lys alone and in pharmaceutical formulations[15] also exhibit biological properties and therapeutic effects. (*R*)-Lys lacks these properties.

The preparation of (*S*)- and (*R*)-Lys solutions and studies of the self-organization and properties of the solutions by physicochemical methods were reported previously[2,3,7] (see Online Supplementary Materials).

A dynamic light scattering (DLS) analysis of the aqueous solutions of **1** and **2** (Figure 1) has revealed that the solutions of both enantiomers are nanoheterogeneous systems similarly to BACs studied previously.[2,3,7] However, the self-organization processes in these solutions in the test concentration range have certain differences.

Judging from the light scattering intensity (*I*) at 1.0 mol dm^{-3} [Figure 1(*a*),(*b*)], domains with sizes (*D*) of about 250 nm predominated in the system based on (*S*)-Lys (93%), whereas particles with diameters around 1 nm predominated in the (*R*)-Lys based system (60%). These particles (micelle-like structures[5]) are dynamic fractal objects mainly consisting of solute (~60%) and water molecules.

On dilution of the (*S*)-Lys based system to 2.5 × 10^{-1}, 1.0 × 10^{-1} mol dm^{-3} and below, the intensity size distribution becomes nearly unimodal, and a unimodal distribution was observed in a range from 1.0 × 10^{-2} to 1.0 × 10^{-7} mol dm^{-3} (see Online Supplementary Materials). The process of self-organization

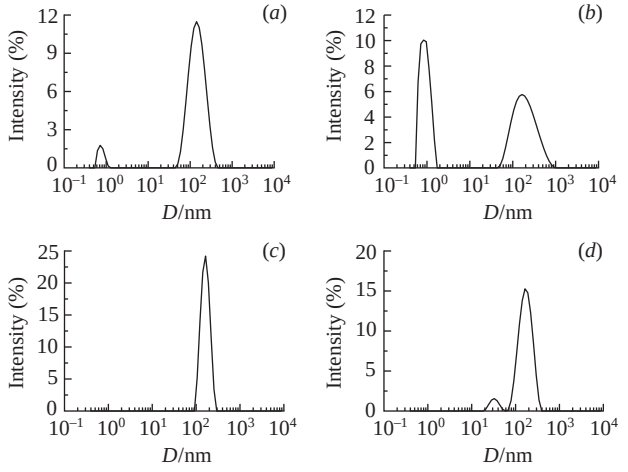

Figure 1 Particle-size (*D*) distribution in aqueous solutions of (*a*),(*c*) (*S*)-Lys and (*b*),(*d*) (*R*)-Lys based on light scattering intensity. Concentration is (*a*),(*b*) 1.0 and (*c*),(*d*) 1.0×10^{-2} mol dm^{-3}, 25 °C.

with dilution was much more complex in systems based on (*R*)-Lys. The particle-size distribution remained bimodal from 1.0×10^{-1} to 1.0×10^{-7} mol dm^{-3} [see Figures 1(*d*) ans S1(*c*)]. A trend towards the formation of larger particles became stronger upon dilution [Figure S2(*c*),(*d*)].

At concentrations of 1.0×10^{-8} and 1.0×10^{-9} mol dm^{-3}, the behaviours of systems based on **1** and **2** were similar: at 1.0×10^{-8} mol dm^{-3} both systems manifested a bimodal distribution, whereas at 1.0×10^{-9} mol dm^{-3} no particles were detected by DLS (silent zone).

From 1.0×10^{-10} mol dm^{-3} and below, like in the high concentration range, some differences were observed in the behaviors of systems based on **1** and **2**. In the case of (*S*)-Lys, particles with sizes of hundreds and thousands nanometers were formed in a range of 1.0×10^{-10}–1.0×10^{-17} mol dm^{-3} [see Figure S1(*b*)], except at 1.0×10^{-15} mol dm^{-3} where no particles were detected. Conversely, in (*R*)-Lys solutions no particles were correctly detected by DLS at 1.0×10^{-9} mol dm^{-3} and below, except for 1.0×10^{-14} mol dm^{-3} [see Figure S1(*d*)]. The feasibility of discrete detection of nanoassociates below the silent zone was shown previously in aqueous systems containing a protein in ultra-high dilution.[16]

A DLS study of systems containing **1** and **2** pre-exposed to hypo-electromagnetic conditions (see Online Supplementary Materials) has shown that no particles are detected below 1.0×10^{-5} mol dm^{-3} in both systems; hence, this is a threshold concentration (c_{th}). Thus, in systems based on (*S*)-Lys, domains are formed in a range of 1.0–1.0×10^{-5} mol dm^{-3}, while nanoassociates are formed in the range of 1.0×10^{-6}–1.0×10^{-17} mol dm^{-3} with two silent zones at 1.0×10^{-9} and 1.0×10^{-15} mol dm^{-3}. The self-organization of systems based on (*R*)-Lys occurs in a more complex way: particles hundreds nm in dimension are formed in a narrower range of low concentrations, namely, domains are formed from 1.0×10^{-2} to 1.0×10^{-5} mol dm^{-3}, whereas nanoassociates are formed from 1.0×10^{-6} to 1.0×10^{-8} mol dm^{-3}. Furthermore, both domains and nanoassociates are formed in systems based on **2** along with dispersed phases of other size ranges (Figures 1, S1, S2), hence the behavior and properties of these systems may depend on a balance between the dispersed phases.

Electrophoretic light scattering (ELS) studies of systems based on (*S*)-Lys have demonstrated that, from 1.0 to 1.0×10^{-17} mol dm^{-3} except for 1.0×10^{-15} and 1.0×10^{-9} mol dm^{-3} (for example, see Figure S3), the ζ-potential of domains and nanoassociates varies nonmonotonously from –24 to –17 mV in the case of domains and from –20 to –1 mV with maxima at 1.0×10^{-7} (–20 mV), 1.0×10^{-10} (–14 mV), 1.0×10^{-12} (–8 mV), 1.0×10^{-14} (–16 mV), and 1.0×10^{-16} (–13 mV) mol dm^{-3} in the case of nanoassociates. In systems based on (*R*)-Lys, the ζ-potential is correctly determined only in a narrow range 1.0×10^{-2}–1.0×10^{-5} mol dm^{-3} where the ζ-potential varies nonmonotonously from –30 to –10 mV.

The UV spectra of aqueous systems contain a broad band at 225–350 nm with a maximum around 270 nm if interfacing *EZ*-water,[17] dissipative water structures,[18] domains and nanoassociates[19] hundreds nm in dimension are formed. These results make it possible to assume that the unusual spectral properties are a distinctive feature of microheterogeneous aqueous systems.

We were the first to study the self-organization and spectral properties of dispersed systems based on (*S*)- and (*R*)-Lys in a concentration range from 1.0×10^{-2} to 1.0×10^{-15} mol dm^{-3} by both DLS and UV spectroscopy methods. This approach was also used to examine the (*S*)- and (*R*)-Lys systems and the solutions of (*S*)-Lys hydrochloride at concentrations from 5.0×10^{-1} to 1.0×10^{-1} mol dm^{-3}. The UV spectra of (*S*)-Lys hydrochloride contained a weak band at 270 nm.[17,20]

The UV spectrum of (*S*)-Lys with a concentration of 0.1 mol dm^{-3} (Figure S4, curve *1*), in which only domains of hundreds nanometres in dimension are formed [Figure S5(*a*)], reveals a band with a shoulder in a range of 250–350 nm with a maximum near 270 nm. In (*S*)-Lys hydrochloride solutions with concentrations from 0.5 to 0.1 mol dm^{-3}, the shoulder at 250–350 nm is missing in the UV spectra (Figure S4, curve *2*), in agreement with previous data,[21] and only micelle-like structures 1.4–1.0 nm in size are formed [Figure S5(*c*)]. Unlike solutions of (*S*)-Lys and (*S*)-Lys hydrochloride where particles of various nature, namely, domains or micelle-like structures with unimodal distribution are formed, which is apparently the reason for dramatic differences in the spectra in a range of 250–350 nm, a bimodal size and volume distribution is observed in (*R*)-Lys systems [see Figures S5(*c*) and S2(*c*)], indicating that particles of both types coexist with predomination of small ones.[22] It is because of this fact that in the case of (*R*)-Lys (see Figure S4, curve *3*), the shoulder in the 250–350 nm range at 0.1 mol dm^{-3} is less distinct than in (*S*)-Lys solutions (see Figure S4, curve *1*). It is likely that the weak band at 270 nm in (*S*)-Lys solutions reported elsewhere[17,20] also results from the formation of an insignificant number of domains in these solutions.

Thus, the data obtained indicate that the appearance of absorbance with a maximum at 270 nm may be due to the ability of systems to form a dispersed phase such as domains hundreds nanometres in dimension containing ordered water and compound molecules, which depends to a considerable extent on the chemical and spatial structure of the compound.

As (*S*)-Lys based systems are diluted, the view of the spectrum changes due to a decrease in absorption in the range of 250–350 nm, which occurs most sharply starting from the 2.5×10^{-2} mol dm^{-3} concentration. At a concentration of 1.0×10^{-2} mol dm^{-3} [Figure 2(*a*), curve *1*] a poorly expressed but statistically reliable absorption region at 215–325 nm is observed, while upon further decrease in concentration to 1.0×10^{-4} mol dm^{-3} [Figure 2(*a*), curve *2*], which is very close to c_{th} (1.0×10^{-5} mol dm^{-3}), there is nearly no absorption in the range of interest.

Thorough measurements of the absorption spectrum [Figure 2(*b*)] of systems based on (*S*)-Lys (1.0×10^{-5}–1.0×10^{-15} mol dm^{-3}) and water obtained using the tenfold dilutions method (blank experiment, see Online Supplementary Materials) showed small but distinct changes in the spectra upon successive dilutions. In a concentration range of 1.0×10^{-5}–1.0×10^{-9} mol dm^{-3}, the absorption bands are nearly the same (curve *1*) and differ from the absorption band of diluted water (curve *5*) by the presence of low-intensity but reliably detectable region at 215–325 nm with a maximum around 225 nm on the shoulder that was repeatedly reproduced in all spectra. However, starting from the concentration of 1.0×10^{-10}

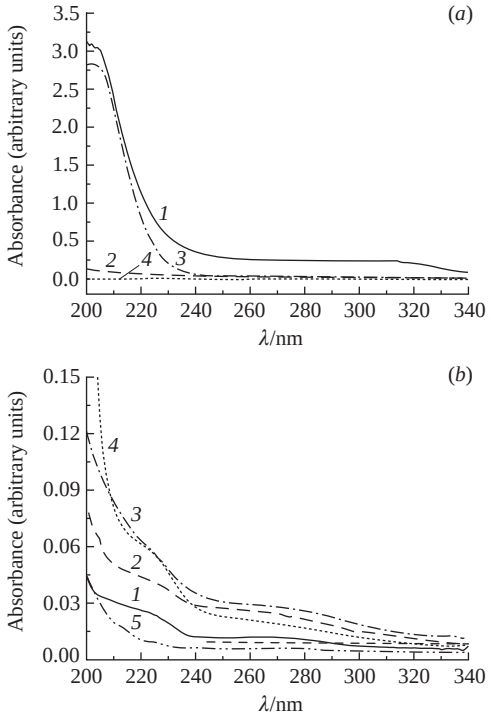

Figure 2 (*a*) Absorption spectra of aqueous systems based on (*a*) (*1*, *2*) (*S*)-Lys and (*3*, *4*) *R*-Lys: (*1*, *3*) 1.0×10^{-2} and (*2*, *4*) 1.0×10^{-4} mol dm^{-3}; (*b*) (*S*)-Lys: (*1*) 1.0×10^{-7}, (*2*) 1.0×10^{-10}, (*3*) 1.0×10^{-12}, (*4*) 1.0×10^{-14} mol dm^{-3} and (*5*) water.

(curve *2*) and down to 1.0×10^{-15} mol dm^{-3}, absorption changes nonmonotonously, increasing most strongly (twofold) near A_{225} at 1.0×10^{-12} and 1.0×10^{-14} mol dm^{-3} (curves *3*, *4*) and decreasing again at 1.0×10^{-11}, 1.0×10^{-13} and 1.0×10^{-15} mol dm^{-3} approximately to the value recorded in the system with 1.0×10^{-7} mol dm^{-3} concentration (curve *1*).

Thus, the appearance of a shoulder near 225 nm is probably due to the formation of nanoassociates that are negatively charged ordered water-molecular structures containing a considerable amount of water,[8] and hence sensitive to changes in physicochemical factors.[2,7,9] In this case, the nonmonotonous variation of A_{225} below 1.0×10^{-5} mol dm^{-3} may be due to changes in the parameters of nanoassociates. In the region of nanoassociate formation, the negative values of the ζ-potential, as described above, and their sizes (Figure 3, curve *1*) vary nonmonotonously with maxima at 1.0×10^{-7}, 1.0×10^{-10}, 1.0×10^{-12} and 1.0×10^{-14} mol dm^{-3}.

At the same concentrations, changes with extrema of the specific electric conductivity of the system (Figure 3) and pH (see Figure S6, curve *2*) were observed. Figure 4 demonstrates the interrelated nonmonotonic concentration dependences of A_{225} and specific electric conductivity (χ) of the system that change symbatically in a concentration range of 1.0×10^{-10}–1.0×10^{-15} mol dm^{-3}. Since the nonmonotonic χ variations in

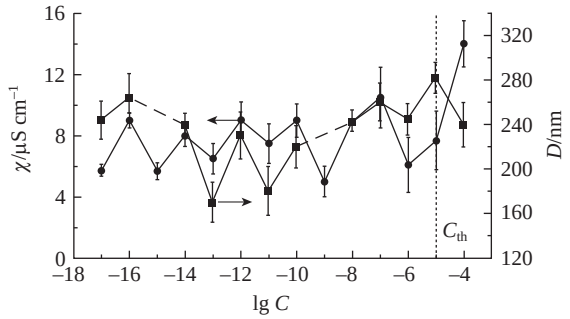

Figure 3 Size (*D*) of particles and electrical conductivity (χ) of aqueous systems based on (*S*)-Lys as a function of concentration, 25 °C.

dispersed low-concentration systems based on BACs are due to rearrangement and nonmonotonic changes in the ζ-potential of nanoassociates,[2,7] the observed picture indicates a regular character and interrelated changes of the parameters of nanoassociates, physicochemical and spectral properties of the system.

A somewhat different picture in the low-concentration region is observed for systems based on (*R*)-Lys [see Figure 2(*a*), curves *3*, *4* and Figure 5]. At concentrations of 1.0×10^{-2}–1.0×10^{-5} mol dm^{-3}, the shoulder in the region of 250–350 nm is missing [Figure 2(*a*), curves *3*, *4*], while starting from 1.0×10^{-6} mol dm^{-3}, a shoulder at 225 nm appears (Figure 5, curves *1*–*5*). As the concentration decreases from 1.0×10^{-7} to 1.0×10^{-15} mol dm^{-3} (curves *2*, *3*), the A_{225} value in this region first increases *ca.* twofold at 1.0×10^{-7}, 1.0×10^{-8} mol dm^{-3} (curves *2*, *3*), then decreases in the entire range studied, 1.0×10^{-9}–1.0×10^{-15} mol dm^{-3} (curve *5*), except at 1.0×10^{-14} mol dm^{-3} (curve *4*).

Thus, the absorption spectra of systems based on (*S*)- and (*R*)-Lys and the nonmonotonic variation of *A* with decreasing concentration show some differences that are related to distinctions in the ability to form domains and nanoassociates. Unlike (*S*)-Lys based systems, in (*R*)-Lys based systems at high concentrations, domains coexist with micelle-like particles that predominate in number[22] (see Figures 1, S1, S2, and S5), as reflected by a much weaker absorption in the range of 250–350 nm in the spectra. However, at concentrations from 1.0×10^{-6} to 1.0×10^{-14} mol dm^{-3}, where nanoassociates are formed in (*R*)-Lys based systems, a shoulder with a maximum near 225 nm comparable to that in (*S*)-Lys systems appears in the UV spectra.

In summary, the configuration of Lys enantiomers considerably affects the capability of systems to form a dispersed phase hundreds nanometres in dimension, *i.e.*, domains and nanoassociates that are composed of ordered water and Lys molecules. Systems based on (*S*)-Lys are superior to those based on (*R*)-Lys in their ability to form domains and to have them converted to nanoassociates in the concentration ranges where such dispersed phases are formed.

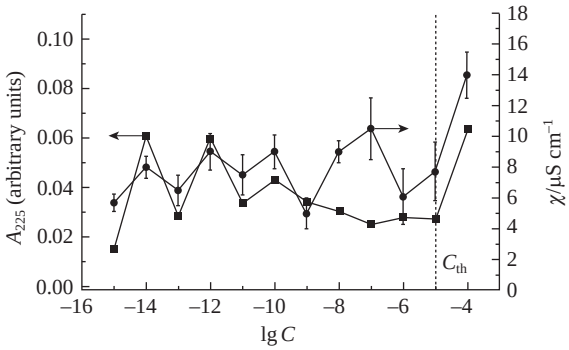

Figure 4 Absorbance at 225 nm (A_{225}) and electrical conductivity (χ) of aqueous systems based on (*S*)-Lys as a function of concentration, 25 °C.

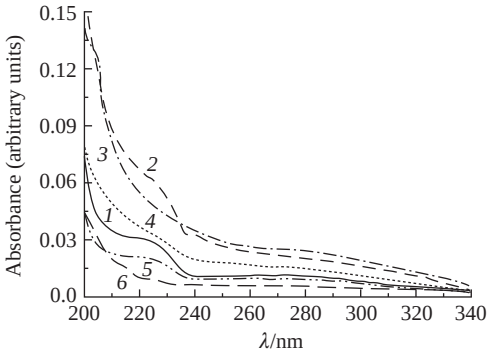

Figure 5 Absorption spectra of aqueous systems based on (*R*)-Lys: (*1*) 1.0×10^{-6}, (*2*) 1.0×10^{-7}, (*3*) 1.0×10^{-8}, (*4*) 1.0×10^{-14}, (*5*) 1.0×10^{-15} mol dm^{-3} and (*6*) water.

This is reflected in the UV absorption spectra as a shoulder appearing in the 215–325 nm region, as non-monotonous variation of A_{225} with concentration, and symbatic changes of parameters of nanoassociates and properties of the systems. The discovered differentiated effect of lysine (*S*)- and (*R*)-enantiomers in a broad concentration range on the self-organization and properties of aqueous systems on their basis may be useful for understanding the phenomena of prime importance in living nature, such as the functional specialization of amino acid enantiomers, in particular, for explaining selective penetration into cells and biological activity at low concentrations of (*S*)-Lys.[17]

We are grateful to S. L. Vasin (KD Sistemy i Oborudovanie) for helpful discussions of ELS measurements and to A. V. Chernova (A. E. Arbuzov Institute of Organic and Physical Chemistry, Kazan Scientific Center, Russian Academy of Sciences) for assistance in studying the UV spectra of solutions.

This study was supported by the Russian Foundation for Basic Research (project no. 16-03-00076).

Online Supplementary Materials

Supplementary data associated with this article can be found in the online version at doi: 10.1016/j.mencom.2018.01.022.

References

1 *Hormesis: A Revolution in Biology, Toxicology and Medicine*, 1st edn., eds. M. P. Mattson and E. J. Calabrese, Humana Press, 2010.
2 A. I. Konovalov and I. S. Ryzhkina, *Geochem. Int*., 2014, **52**, 1207.
3 A. Konovalov, I. Ryzhkina, E. Maltzeva, L. Murtazina, Y. Kiseleva, V. Kasparov and N. Palmina, *Electromagn. Biol. Med*., 2015, **34**, 141.
4 M. Sedlák and D. Rak, *J. Phys. Chem. B*, 2013, **117**, 2495.
5 L. O. Kononov, *RSC Adv*., 2015, **5**, 46718.
6 I. V. Lunev, A. A. Khamzin, I. I. Popov, M. N. Ovchinnikov, I. S. Ryzhkina, O. A. Mishina, Yu. V. Kiseleva and A. I. Konovalov, *Dokl. Phys. Chem*., 2014, **455**, 56 (*Dokl. Akad. Nauk*, 2014, **455**, 656).
7 I. S. Ryzhkina, Yu. V. Kiseleva, O. A. Mishina, L. I. Murtazina, A. I. Litvinov, M. K. Kadirov and A. I. Konovalov, *Russ. Chem. Bull., Int. Ed*., 2015, **64**, 579 (*Izv. Akad. Nauk, Ser. Khim*., 2015, 579).
8 L. N. Gall and N. R. Gall, *Dokl. Phys. Chem*., 2015, **461**, 92 (*Dokl. Akad. Nauk*, 2015, **461**, 673).
9 V. I. Lobyshev, *Ross. Khim. Zh.* (*Zh. Ross. Khim. Ob-va im. D. I. Mendeleeva*), 2007, **51** (1), 107 (in Russian).
10 S. M. Pershin, A. F. Bunkin, M. Ya. Grishin, M. A. Davydov, V. N. Lednev, N. P. Palmina and A. N. Fedorov, *Dokl. Phys*., 2015, **60**, 114 (*Dokl. Akad. Nauk*, 2015, **461**, 160).
11 T. A. Yinnon and Z. Q. Liu, *Water*, 2015, **7**, 70.
12 I. S. Ryzhkina, S. Yu. Sergeeva, E. M. Masagutova, L. I. Murtazina, O. A. Mishina, A. P. Timosheva, V. V. Baranov, A. N. Kravchenko and A. I. Konovalov, *Russ. Chem. Bull., Int. Ed*., 2015, **64**, 2125 (*Izv. Akad. Nauk, Ser. Khim*., 2015, 2125).
13 I. S. Ryzhkina, Yu. V. Kiseleva, L. I. Murtazina, O. A. Mishina, A. P. Timosheva, S. Yu. Sergeeva, V. V. Baranov, A. N. Kravchenko and A. I. Konovalov, *Mendeleev Commun*., 2015, **25**, 72.
14 H. D. Jakubke and H. Jeschkeit, *Aminosäuren, Peptide, Proteine*, Akademie Verlag, Berlin, 1982.
15 S. E. Kondakov, M. Ya. Melnikov and O. S. Prokopzeva, *Dokl. Phys. Chem*., 2014, **455**, 45 (*Dokl. Akad. Nauk*, 2014, **455**, 292).
16 I. S. Ryzhkina, L. I. Murtazina, Yu. V. Kiseleva and A. I. Konovalov, *Dokl. Phys. Chem*., 2015, **462**, 110 (*Dokl. Akad. Nauk*, 2015, **462**, 185).
17 B. H. Chai, J. M. Zheng, Q. Zhao and G. H. Pollak, *J. Phys. Chem. A*, 2008, **112**, 2242.
18 V. Elia, R. Germano and E. Napoli, *Curr. Top. Med. Chem*., 2015, **15**, 559.
19 I. S. Ryzhkina, S. Yu. Sergeeva, R. A. Safiullin, S. A. Ryzhkin, A. B. Margulis, L. I. Murtazina, A. P. Timosheva, A. V. Chernova, M. K. Kadirov and A. I. Konovalov, *Russ. Chem. Bull., Int. Ed*., 2016, **65**, 1505 (*Izv. Akad. Nauk, Ser. Khim*., 2016, 1505).
20 L. Homchaudhuri and R. Swaminathan, *Chem. Lett*., 2001, 844.
21 I. Tinoco, Jr., K. Sauer, J. C. Wang and J. D. Puglisi, *Physical Chemistry: Principles and Applications in Biological Sciences*, 4th edn., Prentice Hall, 2002.
22 *Zetasizer Nano Series. User Manual*, Malvern Instruments, 2008.

Received: 20th April 2017; Com. 17/5230